HHS Public Access

Author manuscript

Ann Thorac Surg. Author manuscript; available in PMC 2022 October 01.

Published in final edited form as:

Ann Thorac Surg. 2021 October ; 112(4): 1317–1324. doi:10.1016/j.athoracsur.2020.07.036.

Dynamic volumetric assessment of the aortic root: The influence of bicuspid aortic valve competence

Alison M. Pouch, Ph.D.[1,2], **Prakash A. Patel, M.D.**[3], **Nimesh D. Desai, M.D., Ph.D.**[4], **Natalie Yushkevich, B.S.**[1], **Michael Goodwin, M.D.**[3], **Eric K. Lai, B.S.**[4], **Albert T. Cheung, M.D.**[5], **Patrick Moeller, M.S.**[4], **Stuart J. Weiss, M.D.**[3], **Joseph H. Gorman III, M.D.**[4], **Joseph E. Bavaria, M.D.**[3], **Robert C. Gorman, M.D.**[4]

[1]Department of Radiology, University of Pennsylvania, Philadelphia, PA

[2]Department of Bioengineering, University of Pennsylvania, Philadelphia, PA

[3]Department of Anesthesiology and Critical Care, University of Pennsylvania, Philadelphia, PA

[4]Division of Cardiovascular Surgery, University of Pennsylvania, Philadelphia, PA

[5]Department of Anesthesiology, Perioperative and Pain Medicine, Stanford University, Stanford, CA

Abstract

Background—Aortic root evaluation is conventionally based on two-dimensional measurements at a single phase of the cardiac cycle. This work presents an image analysis method for assessing dynamic three-dimensional changes in the aortic root of minimally calcified bicuspid aortic valves (BAVs) with and without moderate to severe aortic regurgitation.

Methods—The aortic root was segmented over the full cardiac cycle in three-dimensional transesophageal echocardiographic images acquired from 19 patients with minimally calcified BAVs and from 16 patients with physiologically normal tricuspid aortic valves (TAVs). The size and dynamics of the aortic root were assessed using the following image-derived measurements: absolute mean root volume and mean area at the level of the ventriculoaortic junction, sinuses of Valsalva, and sinotubular junction, as well as normalized root volume change and normalized area change of the ventriculoaortic junction, sinuses of Valsalva, and sinotubular junction over the cardiac cycle.

Results—Normalized volume change over the cardiac cycle was significantly greater in BAV roots with moderate to severe regurgitation than in normal TAV roots and in BAV roots with no or mild regurgitation. Aortic root dynamics were most significantly different at the mid-level of the sinuses of Valsalva in BAVs with moderate to severe regurgitation than in competent TAVs and BAVs.

Corresponding author: Alison M. Pouch, Ph.D., Assistant Professor of Radiology and Bioengineering, University of Pennsylvania, 3700 Hamilton Walk, Office D606, Philadelphia, PA 19104, pouch@pennmedicine.upenn.edu.

Conclusions—Echocardiographic reconstruction of the aortic root demonstrates significant differences in dynamics of BAV roots with moderate to severe regurgitation relative to physiologically normal TAVs and competent BAVs. This finding may have implications for risk of future dilatation, dissection, or rupture, which warrant further investigation.

Keywords

aortic root; congenital heart disease; echocardiography; imaging

Normal structure and function of the aortic root optimize transvalvular flow and minimize stresses on the aortic cusps. As such, surgical interventions of the aortic valve must account for evaluation of the aortic root, especially in the presence of a bicuspid aortic valve (BAV), which is associated with a high prevalence of valvular dysfunction and aortic abnormalities[1]. In clinical practice, aortic root assessment is conventionally based on 2D measurement of root diameters at a single phase of the cardiac cycle. Recent work has demonstrated the disadvantages of conventional single-plane diameter measurements[2] and has emphasized the benefits of a more comprehensive 3D aortic root analysis with 3D transesophageal (3D TEE) imaging[3]. Aortic root sizing with 3D TEE has been compared to other imaging modalities such as multidetector computed tomography[4,5], with particular emphasis on planning transcatheter aortic valve replacement for treatment of aortic stenosis[6,7]. While these studies have focused on static aortic root geometry in predominantly calcified aortic valves, much of our knowledge of aortic root *dynamics* over the cardiac cycle in non-calcified valves has been gained through invasive marking strategies in animal models[8,9]. Although some human imaging studies have analyzed aortic root dynamics in minimally calcified BAV patients[10], it is not known how volumetric aortic root dynamics differs in patients with physiologically normal tricuspid aortic valves (TAVs) and in those with minimally calcified BAVs. Such knowledge is relevant to prediction, diagnosis, and treatment of aortic regurgitation (AR) and aortopathies in BAV patients.

Towards this goal, this work presents a custom 4D (3D + time) image analysis method for volumetrically assessing aortic root dynamics of minimally calcified TAVs and BAVs over the cardiac cycle. The objectives of this study are two-fold: to semi-automatically obtain 4D patient-specific models of the aortic root from real-time 3D TEE in order to measure aortic root areas and volume over the cardiac cycle, and to test the hypothesis that abnormalities in the dynamics of minimally calcified BAV roots are associated with the presence of AR.

Patients and Methods

Image Data and Patient Population

This study was approved by the Institutional Review Board at the University of Pennsylvania. Electrocardiographically gated real-time 3D TEE images of the aortic root were retrospectively acquired from routine intra-operative exams of 35 patients performed immediately before cardiac procedure. The patients included 16 with physiologically normal TAVs and ascending aortas and 19 with minimally calcified BAVs with or without aneurysm of the aortic root and/or ascending aorta. The 3D TEE images were devoid of stitching artifacts and the entire aortic root remained in the field of view during acquisition. The

images were obtained using the iE33 imaging platform (Philips Medical Systems, Andover, MA) with a 2 – 7 MHz matrix-array transducer at end-expiration during positive pressure ventilation in anesthetized patients to eliminate motion caused by respiration. Images were acquired in full volume mode and averaged over four consecutive heart beats. Each patient's 3D TEE image series consisted of 9 to 36 frames showing the aortic root from the level of the ventriculoaortic junction (VAJ) to the sinotubular junction (STJ) over one complete cardiac cycle beginning at early systole. The images were exported in Cartesian format with nearly isotropic resolution ranging from 0.4 to 0.8 mm. Intraoperative AR was assessed by board-certified echocardiographers using the American Society of Echocardiography and Society of Cardiovascular Anesthesiologists guidelines for performing a comprehensive transesophageal echocardiographic exam[11,12]. In this study, the BAV group was divided into two AR severity categories: none-to-mild and moderate-to-severe. Clinical characteristics of the study population, as well as BAV subgroup characteristics related to AR severity, the presence of dilatation or aneurysm of the aortic root and/or ascending aorta, and cusp morphology are presented in Table 1. The BAV subgroup with moderate to severe AR was younger in age and predominantly male. The three subgroups did not otherwise differ in terms of body mass index and mean systolic or diastolic blood pressure.

4D Image Segmentation of the Aortic Root

From each patient's 3D TEE dataset, a series of 3D aortic root reconstructions was generated over one cardiac cycle using the custom semi-automated image analysis pipeline illustrated in Figure 1. Briefly, the aortic root was first manually traced in a systolic frame of the cardiac cycle using ITK-SNAP, an open-source tool for interactive 3D medical image segmentation[13]. The segmentation was annotated at the level of the STJ and the VAJ to define the orientation of the root for subsequent measurement. This segmentation was referred to as the "reference segmentation" and was verified by a second observer. Deformable registration (image warping) between consecutive frames was performed with the open-source *greedy* 3D registration tool[14] in order to propagate the reference segmentation to all other frames of the TEE series. The result was a series of 3D segmentations of the aortic root at all available frames in the cardiac cycle. A triangulated mesh of each segmentation was automatically generated from the surface of each segmentation using an adaptation of [15], such that automated measurements of root area and volume could be automatically computed. This series of anatomical meshes is referred to as a 4D patient-specific model of the aortic root.

The image analysis pipeline is referred to as semi-automated since it involved an observer tracing the aortic root manually in one 3D frame. All subsequent steps, including propagation of the reference segmentation to all image frames and computation of aortic root measurements, were fully automated. Without the fully automated propagation and computation steps, the manual requirements would be enormously greater since there are generally tens of 3D frames in each data series.

Quantitative Root Analysis

Measurements were automatically computed from the aortic root meshes as follows. The mesh was sliced at eight equally spaced levels of the aortic outflow tract from the VAJ to

STJ as illustrated in Figure 2a. At each level, the area enclosed by the inner wall of the root was computed. The normalized area change over the cardiac cycle at each level of the aortic root was calculated as:

$$\text{normalized area change (\%)} = 100 \cdot \frac{\text{maximum root area (mm}^2\text{)} - \text{minimum root area (mm}^2\text{)}}{\text{minimum root area (mm}^2\text{)}}$$

Aortic root volume was calculated as the integral of the area of each slice multiplied by the space between slices. The normalized root volume change over the cardiac cycle was computed as follows:

$$\text{normalized volume change (\%)} = 100 \cdot \frac{\text{maximum root volume (mL)} - \text{minimum root volume (mL)}}{\text{minimum root volume (mL)}}$$

Stroke volume (SV) was estimated as SV = CI·BSA/HR, where CI is the cardiac index, BSA is body surface area, and HR is heart rate in the echocardiogram. Here, a low-normal CI of 2.3 L/min/m^2 was assumed since all patients were in an anesthetized state and it is the approximate flow rate maintained during cardiopulmonary bypass[16]. The stroke volume buffer was calculated as the change in root volume divided by estimated stroke volume.

Statistical Analysis

Continuous variables were reported as the mean ± standard deviation for measurements with a normal distribution or as the median and interquartile range for non-normal distributions. Normality was evaluated with the Shapiro-Wilk test. The measurements tested were mean root volume; mean root area at the level of the VAJ, SOV, and STJ; normalized volume change; normalized area change of the VAJ, SOV, and STJ; estimated stroke volume; and stroke volume buffer. These measurements were compared between TAVs, BAVs with no-to-mild AR, and BAVs with moderate-to-severe AR using one-way ANOVA. For normally distributed continuous variables, group comparisons were made with the analysis of variance test and pairwise post-hoc comparisons with Bonferroni correction for multiple testing. For variables with non-normal distributions, the Kruskal-Wallis and Dunn tests for pairwise comparisons with the Bonferroni correction were used. A repeated measures ANOVA with a between subjects term was used to compare normalized area changes of the same valvular groups at all eight aortic root levels measured.

Results

A total of 835 individual 3D aortic root models were generated from the 3D TEE image series of 35 patients. On average, 23 aortic root models were generated per patient over one cardiac cycle. Sample aortic root models from four BAV patients are illustrated in Figure 3, and a 4D model of a BAV root over the cardiac cycle is shown in a supplemental video. The variation in size of the BAV roots can be qualitatively observed, as the BAV group included a mix of patients with and without dilatation or aneurysm of the aortic root and/or ascending aorta and with AR ranging from none to severe. As shown in the three right-most BAV roots

in Figure 3, the moderate-to-severe AR group included a mix of roots whose size ranged from normal to aneurysmal.

Absolute mean root volume and areas, as well as normalized root volume and area changes over the cardiac cycle, are presented in Table 2 and are illustrated in Figure 2b, Figure 4, and Figure 5, stratified by group: all TAVs, BAVs with no-to-mild AR, and BAVs with moderate-to-severe AR. In terms of aortic root size, the absolute volume and area measurements were highly variable in BAVs since the subgroups consisted of both non-dilated and aneurysmal phenotypes as summarized in Table 1. The mean aortic root volume was nearly significantly different between the three subgroups ($p = 0.0523$). Mean root area was found to be significantly higher in BAVs with moderate-to-severe AR relative to the TAV controls at the level of the STJ ($p = 0.0026$), SOV ($p = 0.032$), and VAJ ($p = 0.0035$). Mean STJ area was also significantly greater in BAVs with no-to-mild AR relative to TAV controls ($p = 0.0052$). Differences in absolute root volume, and STJ, SOV, and VAJ areas were not significant between BAV subgroups.

In terms of aortic root dynamics, normalized change in volume over the cardiac cycle was significantly different in the TAV group, the BAV group with minimal AR, and the BAV group with moderate to severe AR ($p = 0.0026$). In pairwise comparisons, the normalized volume change in BAV roots with moderate to severe AR was significantly greater than that in TAV roots with no AR ($p=0.0043$) and in BAV roots with no to mild AR ($p=0.0347$) as shown in Figure 4.

Normalized area change was significantly different between groups at the level of the SOV ($p = 0.0005$) and STJ ($p = 0.0042$), but not at the level of the VAJ ($p = 0.493$). Illustrated in Figure 5, post-hoc pairwise comparisons showed that normalized SOV area change in the moderate-to-severe AR group was significantly higher than both the TAV group ($p = 0.009$) and BAV group with minimal AR ($p = 0.0014$), but was not significantly different between TAVs and the BAV group with minimal AR ($p=0.581$). Relative to TAV controls, the BAVs with moderate to severe AR had significantly elevated stroke volume ($p = 0.012$) and stroke volume buffer ($p = 0.0245$). The estimated stroke volume and stroke volume buffer were not significantly different between BAV subgroups.

To analyze root dynamics trends along the length of the outflow tract, repeated measures ANOVA with a between-subjects term for valve type showed that the normalized root area change (Figure 2b) was significantly different between BAV subgroups ($p = 0.012$) and between TAV controls and BAVs with moderate to severe AR ($p = 0.024$). Normalized root area changes in BAVs with no to mild AR were not significantly different with respect to TAV controls ($p = 0.967$). The trends in Figure 2b illustrate that the largest normalized area changes occur at the level of the VAJ, with smaller root area changes at the level of the SOV.

Comment

This study demonstrates a semi-automated method for creating 4D patient-specific models of minimally calcified aortic roots from intra-operative TEE data. It is the first to analyze aortic root volume changes over the cardiac cycle, particularly in patients with minimally calcified BAVs. While aortic root assessment is conventionally based on diameter

measurements made at different levels of the outflow tract, aortic root volume is a global measure of size that does not assume root symmetry. Root volume can also be interpreted in conjunction with root area measurements made at multiple levels of the outflow tract (STJ, SOV, and VAJ), which taken together capture both the size of the root and characterization of the root phenotype. In terms of aortic root dynamics, an advantage of computing *normalized* root volume change in addition to absolute size measurements is that it is independent of patient habitus (aortic size is known to vary in patients with respect to BSA[17]) and the presence of a root aneurysm (since absolute change in volume may be related to the size of the root). In summary, the image analysis strategy presented in this work facilitates computation of both absolute and normalized root size change, both of which are important in clinical decision making.

The analysis of root area changes in Figure 2b and Figure 5 indicates that root dynamics over the cardiac cycle differs along the length of the aortic root; the greatest change in root size over the cardiac cycle generally occurs at the level of the VAJ. This finding was observed in all subgroups in this study. A primary finding of this study is that BAV roots with moderate to severe AR are not only larger than physiologically normal TAVs, but they also have a significantly increased normalized root volume change over the cardiac cycle relative to the aortic roots of normal TAVs and of minimally calcified BAVs with minimal AR. The increased normalized root volume change in severely regurgitant BAVs may be attributable to enhanced dynamics at the level of the SOV observed in this subgroup (Figure 5, right column). Given that the estimated stroke volume and stroke volume buffer were higher in BAVs with moderate-to-severe AR relative to the minimal AR subgroups, it is conceivable that the elevated stroke volume of BAVs with severe AR is, in part, accommodated by increased root volume change over the cardiac cycle. These findings have not been previously reported and may have implications for AR predisposition and risk for future aortic dilatation, dissection, or rupture, which warrant further investigation.

This study has several limitations. Considering the morphological heterogeneity of BAVs, further studies with larger sample sizes (including more physiologically normal BAVs, in particular) are needed to investigate the association between BAV root dynamics and valve competence, cusp morphology, root asymmetry, vascular stiffness, and patterns of aortopathy. While the results indicate that root dynamics are altered in BAVs with moderate to severe AR relative to competent aortic valves, this finding does not indicate whether changes in root dimensions are a cause for AR or the result of AR. In addition, while the 3D multiplanar measurements presented in this study overcome pitfalls of conventional 2D root measurements, the proposed 4D TEE analysis has not been compared to conventional 2D analysis or other modalities such as multidetector computed tomography. This study also used to a low-normal estimation of cardiac output to approximate stroke volume, which may have underestimated stroke volume in patients with severe AR. Further research will be needed to address these questions. The image analysis methodology presented in this work is an important step towards accomplishing these future goals.

In conclusion, this study presents a semi-automated strategy for visualizing and numerically evaluating the dynamic geometry of the aortic root as it evolves over the cardiac cycle, which can be standardized to provide more information than traditional methods for

derivation of static 2D aortic root diameters. This work may potentially lead to new user-friendly and cost-effective strategies for risk stratification and surgical management of patients with minimally calcified aortic valves.

Supplementary Material

Refer to Web version on PubMed Central for supplementary material.

Abbreviations

3D	three-dimensional
4D	three-dimensional (3D) + time
BAV	bicuspid aortic valve
TAV	tricuspid aortic valve
TEE	transesophageal echocardiography
AR	aortic regurgitation
VAJ	ventriculoaortic junction
SOV	sinuses of Valsalva
STJ	sinotubular junction

References

[1]. Norton E, Yang B. Managing Thoracic Aortic Aneurysm in Patients with Bicuspid Aortic Valve Based on Aortic Root-Involvement. Front Physiol. 2017;8:397. [PubMed: 28659818]

[2]. Plonek T, Berezowski M, Bochenek M, Filip G, Rylski B, Golesworthy T, Jasinski M. A comparison of aortic root measurements by echocardiography and computed tomography. J Thorac Cardiovasc Surg. 2019;157(2):479–86. [PubMed: 30227996]

[3]. Hagendorff A, Evangelista A, Fehske W, Schafers HJ. Improvement in the Assessment of Aortic Valve and Aortic Aneurysm Repair by 3-Dimensional Echocardiography. JACC Cardiovasc Imaging. 2019;12(11 Pt 1):2225–44. [PubMed: 30878428]

[4]. Rodriguez-Palomares JF, Teixido-Tura G, Galuppo V, Cuellar H, Laynez A, Gutierrez L, Gonzalez-Alujas MT, Garcia-Dorado D, Evangelista A. Multimodality Assessment of Ascending Aortic Diameters: Comparison of Different Measurement Methods. J Am Soc Echocardiogr. 2016;29(9):819–26. [PubMed: 27288090]

[5]. Calleja A, Thavendiranathan P, Ionasec RI, Houle H, Liu S, Voigt I, Sai Sudhakar C, Crestanello J, Ryan T, Vannan MA. Automated quantitative 3-dimensional modeling of the aortic valve and root by 3-dimensional transesophageal echocardiography in normals, aortic regurgitation, and aortic stenosis: comparison to computed tomography in normals and clinical implications. Circ Cardiovasc Imaging. 2013;6(1):99–108. [PubMed: 23233743]

[6]. Queiros S, Morais P, Dubois C, Voigt JU, Fehske W, Kuhn A, Achenbach T, Fonseca JC, Vilaca JL, D'Hooge J. Validation of a Novel Software Tool for Automatic Aortic Annular Sizing in Three-Dimensional Transesophageal Echocardiographic Images. J Am Soc Echocardiogr. 2018;31(4):515–25. [PubMed: 29625649]

[7]. Mediratta A, Addetia K, Medvedofsky D, Schneider RJ, Kruse E, Shah AP, Nathan S, Paul JD, Blair JE, Ota T, Balkhy HH, Patel AR, Mor-Avi V, Lang RM. 3D echocardiographic analysis of aortic annulus for transcatheter aortic valve replacement using novel aortic

valve quantification software: Comparison with computed tomography. Echocardiography. 2017;34(5):690–9. [PubMed: 28345211]

[8]. Lansac E, Lim HS, Shomura Y, Lim KH, Rice NT, Goetz W, Acar C, Duran CM. A four-dimensional study of the aortic root dynamics. Eur J Cardiothorac Surg. 2002;22(4):497–503. [PubMed: 12297162]

[9]. Cheng A, Dagum P, Miller DC. Aortic root dynamics and surgery: from craft to science. Philos Trans R Soc Lond B Biol Sci. 2007;362(1484):1407–19. [PubMed: 17594968]

[10]. Shibayama K, Harada K, Berdejo J, Tanaka J, Mihara H, Itabashi Y, Shiota T. Comparison of aortic root geometry with bicuspid versus tricuspid aortic valve: real-time three-dimensional transesophageal echocardiographic study. J Am Soc Echocardiogr. 2014;27(11):1143–52. [PubMed: 25155517]

[11]. Hahn RT, Abraham T, Adams MS, Bruce CJ, Glas KE, Lang RM, Reeves ST, Shanewise JS, Siu SC, Stewart W, Picard MH. Guidelines for performing a comprehensive transesophageal echocardiographic examination: recommendations from the American Society of Echocardiography and the Society of Cardiovascular Anesthesiologists. J Am Soc Echocardiogr. 2013;26(9):921–64. [PubMed: 23998692]

[12]. Zoghbi WA, Enriquez-Sarano M, Foster E, Grayburn PA, Kraft CD, Levine RA, Nihoyannopoulos P, Otto CM, Quinones MA, Rakowski H, Stewart WJ, Waggoner A, Weissman NJ, American Society of E. Recommendations for evaluation of the severity of native valvular regurgitation with two-dimensional and Doppler echocardiography. J Am Soc Echocardiogr. 2003;16(7):777–802. [PubMed: 12835667]

[13]. Yushkevich PA, Piven J, Hazlett HC, Smith RG, Ho S, Gee JC, Gerig G. User-guided 3D active contour segmentation of anatomical structures: significantly improved efficiency and reliability. Neuroimage. 2006;31(3):1116–28. [PubMed: 16545965]

[14]. Yushkevich PA, Pluta J, Wang H, Wisse LE, Das S and Wolk D Fast Automatic Segmentation of Hippocampal Subfields and Medial Temporal Lobe Subregions in 3 Tesla and 7 Tesla MRI. Alzheimer's & Dementia: The Journal of the Alzheimer's Association, 2016; 12(7):126–127. (open-source code available on GitHub: https://github.com/pyushkevich/greedy)

[15]. Pouch AM, Yushkevich PA, Aly AH, Woltersom AHF, Okon E, Aly AH, Yushkevich N, Parameshwaran S, Wang J, Oguz B, Gee JC, Oguz I, Schwartz N. Automated Meshing of Anatomical Shapes for Deformable Medial Modling: Application to the Placenta in 3D Ultrasound. 2020 IEEE 17th International Symposium on Biomedical Imaging, Iowa City, 2020; 1842–1846.

[16]. Murphy GS, Hessel EA, Groom RC. Optimal Perfusion During Cardiopulmonary Bypass: An Evidence-Based Approach. Anesthesia & Analgesia2009;108(5):1394–1417. [PubMed: 19372313]

[17]. Devereux RB, de Simone G, Arnett DK, Best LG, Boerwinkle E, Howard BV, Kitzman D, Lee ET, Mosley TH Jr., Weder A, Roman MJ. Normal limits in relation to age, body size and gender of two-dimensional echocardiographic aortic root dimensions in persons >/=15 years of age. Am J Cardiol. 2012;110(8):1189–94. [PubMed: 22770936]

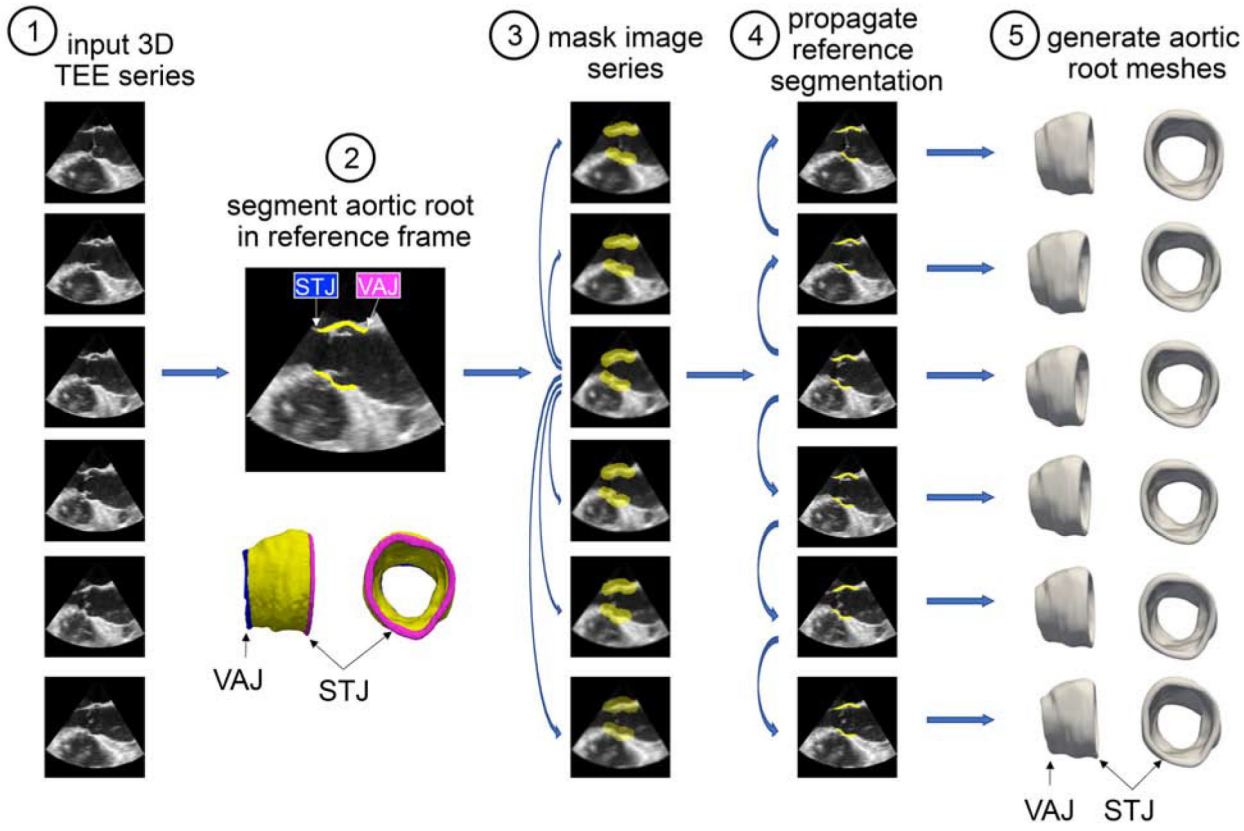

Figure 1:

Semi-automated method for creating 4D aortic root reconstructions from real-time 3D TEE image data: (1) Real-time 3D TEE images were acquired over the cardiac cycle. (2) The aortic root was manually traced in a systolic frame of the cardiac cycle. This "reference" segmentation was annotated at the level of the STJ and the VAJ to define the orientation of the root for subsequent measurement. (3) A dilated mask of the reference segmentation was generated to create a region of interest around the aortic root in the reference frame. The TEE image series was down-sampled, and deformable registration between each consecutive pair of 3D volumes was performed. The resulting deformation fields were used to propagate the reference mask to all 3D volumes in the series. (4) The reference frame was registered at full resolution to all other 3D volumes in the TEE series using the reference mask for increased computational efficiency and precision. The result was a series of 3D segmentations of the aortic root at all available frames in the cardiac cycle. (5) A triangulated mesh of each segmentation was automatically generated from the surface of each segmentation such that automated measurements of root area and volume could be computed.

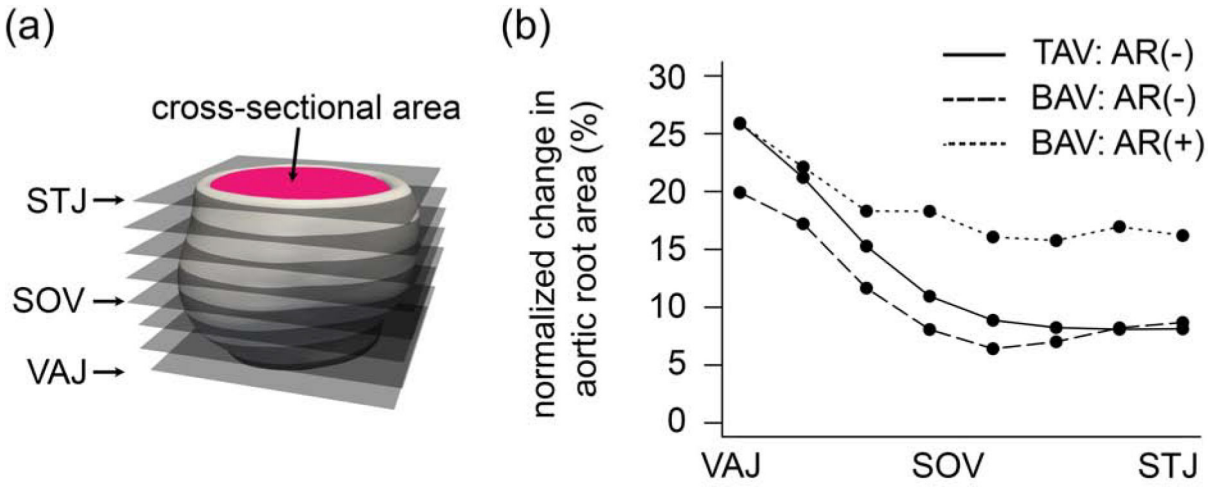

Figure 2:

(a) The aortic root is sliced at 8 levels from the VAJ to STJ and cross-sectional area of the inner wall of the root is computed at each level. Root volume is the total volume between the VAJ and STJ levels. (b) Normalized mean area change over the cardiac cycle is plotted as a function of normalized distance along the aortic root from the VAJ to STJ. Individual curves are shown for TAVs, BAVs with no to mild AR, and BAVs with moderate to severe AR. (VAJ = ventriculoaortic junction, STJ = sinotubular junction)

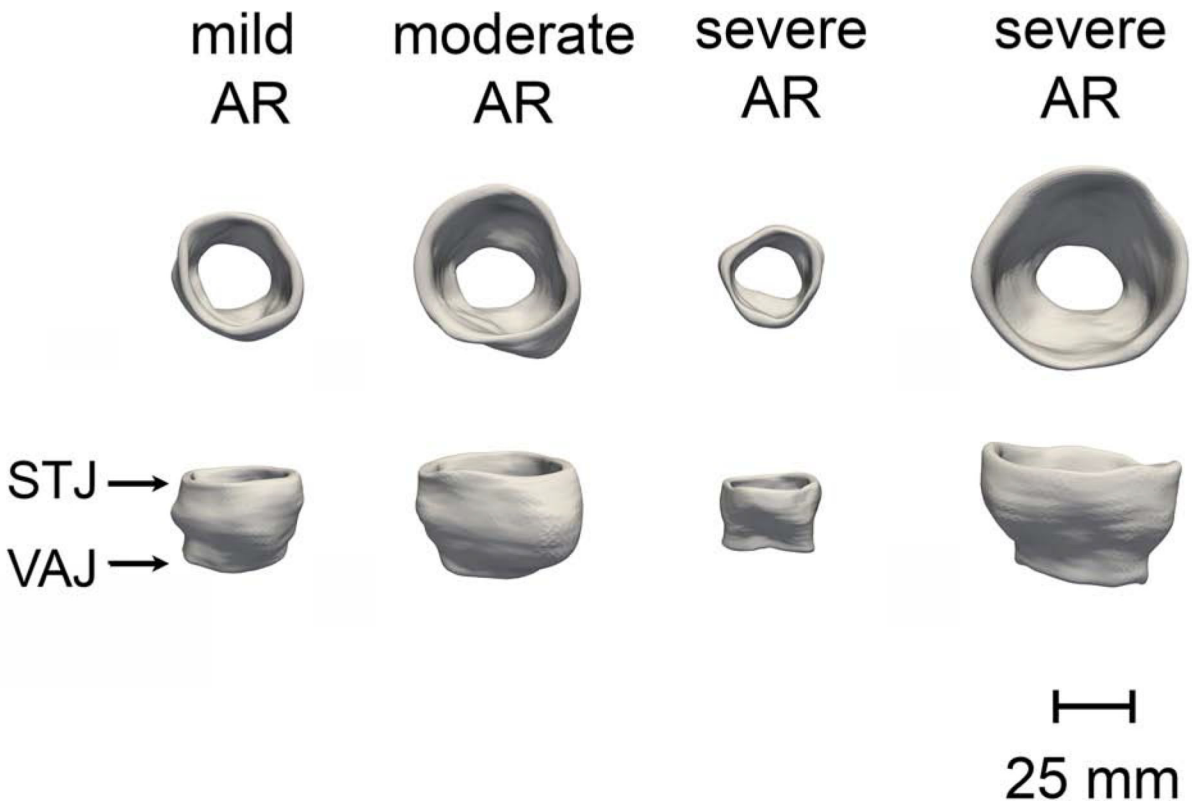

Figure 3:
3D TEE image-derived models of the aortic root from four subjects with BAVs and varying degrees of AR severity. (VAJ = ventriculoaortic junction, STJ = sinotubular junction)

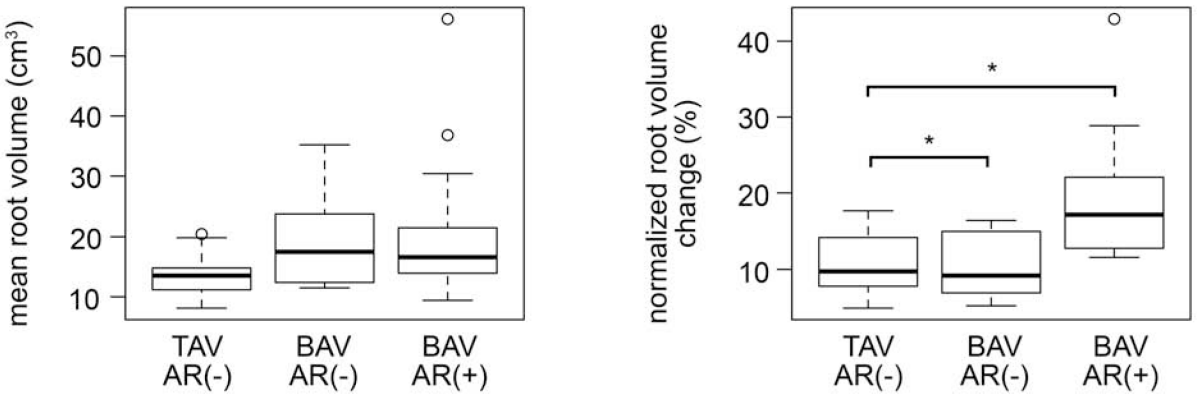

Figure 4:

Normalized aortic root volume change over the cardiac cycle for TAVs (denoted as TAV AR(−)), BAVs with no to mild AR (denoted as BAV AR(−)), and BAVs with moderate to severe AR (denoted as BAV AR(+)).

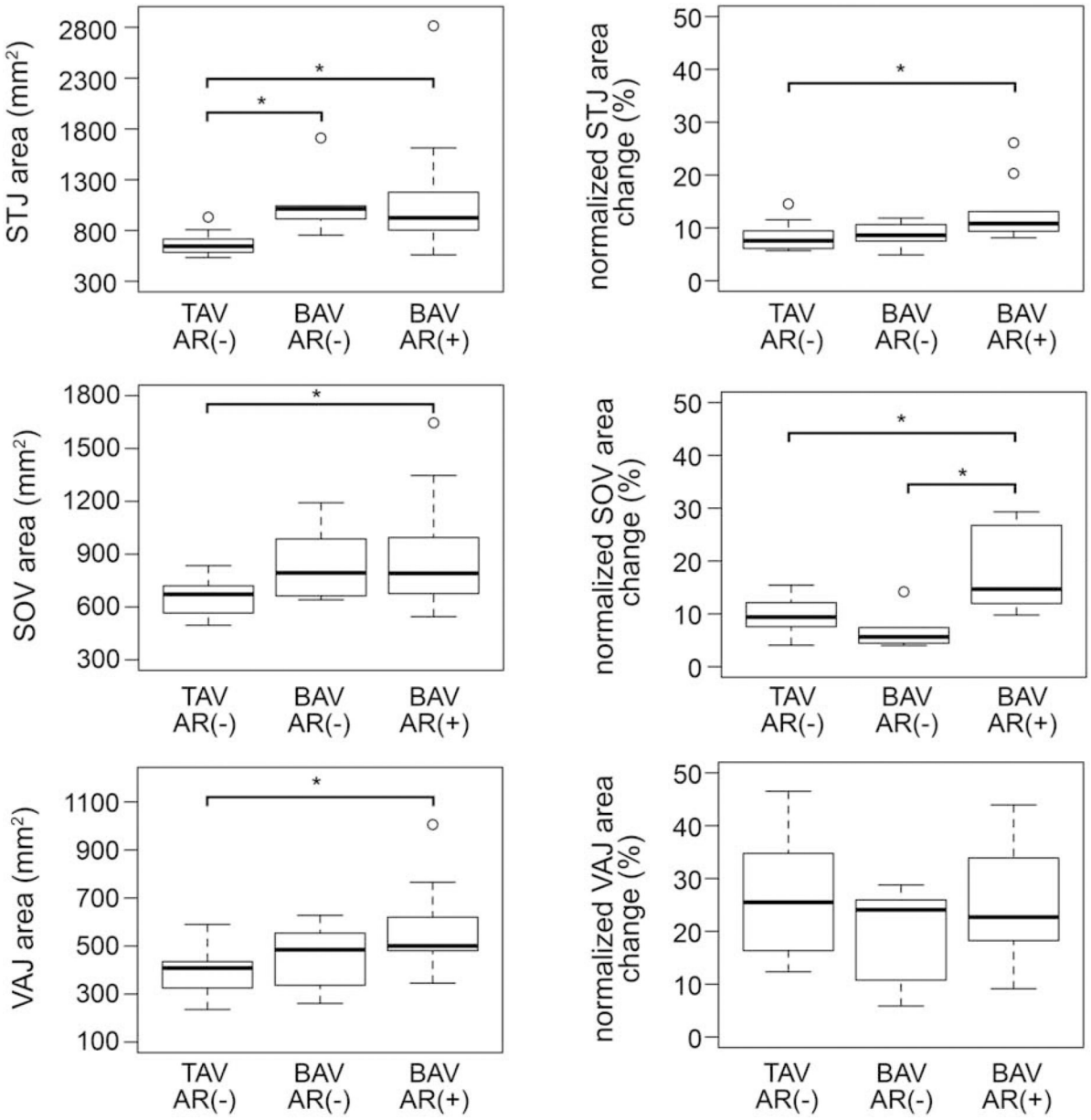

Figure 5:

Normalized change in area of the aortic root over the cardiac cycle at the level of the VAJ (ventriculoaortic junction), SOV (sinuses of Valsalva), and STJ (sinotubular junction) for patients with physiologically normal TAVs (denoted as TAV AR(−)), BAVs with no to mild AR (denoted as BAV AR(−)), and moderate to severe AR (denoted as BAV AR(+)).

Table 1:

Clinical characteristics and aortic valve characteristics related to AR severity, the presence of dilatation or aneurysm of the aortic root and/or ascending aorta, and cusp fusion pattern.

	All TAVs (N = 16)	BAVs: no to mild AR (N = 6)	BAVs: moderate to severe AR (N = 13)
Age (years)	61 ± 12	51 ± 24	46 ± 12
Total females (%)	7 (44)	2 (33)	4 (29)
Body mass index (kg/m^2)	27.8 ± 5	23.6 ± 6	26.2 ± 4
Systolic blood pressure (mmHg)	128 ± 14	135 ± 17	137 ± 18
Diastolic blood pressure (mmHg)	76 ± 12	78 ± 11	69 ± 16
Aortic valve characteristics (total per group):			
Physiologically normal	16	1	0
AR only	0	0	5
Dilatation or aneurysm of the ascending aorta and/or root	0	5	9
L–R coronary cusp fusion (Sievers Type 1)	—	3	7

Table 2:

3D TEE-derived aortic root volume measurements.

	All TAVs (N = 16)	BAVs: no to mild AR (N = 6)	BAVs: moderate to severe AR (N = 13)
Mean root volume (mL)	13.5 (3.2)	17.5 (10.0)	16.6 (7.6)
Normalized root volume change (%)	9.7 (6.2)	9.2 (6.2)	17.2 (9.3) *†
Mean VAJ area (mm^2)	390 ± 93	458 ± 137	571 ± 177 *
Normalized VAJ area change (%)	25.9 ± 10.6	19.9 ± 9.3	25.9 ± 12.3
Mean SOV area (mm^2)	659 ± 103	845 ± 218	889 ± 324 *
Normalized SOV area change (%)	9.4 (4.2)	5.6 (2.4)	14.7 (14.7) *†
Mean STJ area (mm^2)	545 (121)	913 (110) *	824 (373) *†
Normalized STJ area change (%)	7.6 (3.3)	8.6 (2.6)	10.8 (3.7) *
Estimated stroke volume (mL)	59.7 ± 13.0	77.5 ± 21.8	89.3 ± 36.7 *
Stroke volume buffer (%)	2.1 (0.9)	2.2 (3.1)	3.1 (2.8) *

Mean and normalized values are computed over the full cardiac cycle (* denotes $p < 0.05$ with respect to all TAVs, † denotes $p < 0.05$ with respect to BAVs with no to mild AR)